Published in final edited form as:

Adv Opt Mater. 2022 August 04; 10(15): . doi:10.1002/adom.202200242.

True FRET-based sensing of pH via Separation of FRET and Photon Reabsorption

Conrad Corbella Bagot[1,†], **Eric Rappeport**[1,†], **Ananda Das**[2,†], **Taleb BaTis**[3], **Wounjhang Park**[*,1,3]

[1]University of Colorado, Department of Electrical, Computer, and Energy Engineering

[2]University of Colorado, Department of Physics

[3]University of Colorado, Materials Science and Engineering Program

Abstract

Förster Resonance Energy Transfer (FRET)-based devices have been extensively researched as potential biosensors due to their highly localized responsivity. In particular, dye-conjugated upconverting nanoparticles (UCNPs) are among the most promising FRET-based sensor candidates. UCNPs have a multi-modal emission profile that allows for ratiometric sensing, and by conjugating a biosensitive dye to their surface, this profile can be used to measure localized variations in biological parameters. However, the complex nature of the UCNP energy profile as well as reabsorption of emitted photons must be taken into account in order to properly sense the target parameters. To our knowledge, no proposed UCNP-based sensor has accurately taken care of these intricacies. In this article, we account for these complexities by creating a FRET-based sensor that measures pH. This sensor utilizes Thulium (Tm^{3+})-doped UCNPs and the fluorescent dye Fluorescein Isothiocyanate (FITC). We first demonstrate that photon reabsorption is a serious issue for the 475 nm Tm^{3+} emission, thereby limiting its use in FRET-based sensing. We then show that by taking the ratio of the 646 and 800 nm emissions rather than the more popular 475 nm one, we are able to measure pH exclusively through FRET.

1 Introduction

Conventional biosensing techniques rely on measuring ensemble-averaged properties to discern important information about the cellular environment. Such techniques are inherently limited in their spatial resolution and cannot give clear information about the local medium surrounding a single cell. There is thus a need to develop new sensors that can distinguish physiological parameters such as pH, temperature, pressure, and molecular concentrations on the cellular or sub-cellular level [1, 2]. Among the most promising sensors being developed are those that rely on Förster Resonance Energy Transfer (FRET). FRET is a non-radiative process where energy can be transferred from a donor (ion or molecule) to an

*Corresponding author: won.park@colorado.edu.
†These authors contributed equally.

Supplementary Information

Supplementary Information is available from the Wiley Online Library or from the author.

acceptor [3, 4, 5]. The rate of this exchange is highly distance-dependent and fades rapidly with increasing donor-acceptor separation. Thus sensors that utilize FRET are capable of measuring local variations in critical biological parameters.

Of the possible FRET-based sensors, those based off of upconverting nanoparticles (UCNPs) are among the most promising. UCNPs are unique nanoparticles that can emit at several distinct visible wavelengths from a single, near-infrared excitation source. UCNPs exhibit many advantageous characteristics for bioimaging and sensing such as no photobleaching, no blinking, and no background autofluorescence [6, 7]. In particular, many groups have attempted to utilize UCNPs as a FRET-based sensor by conjugating a fluorescent dye to the UCNP surface [8, 9, 10, 11, 12, 13, 14, 15, 16, 17, 18, 19, 20, 21, 22, 23, 24, 25]. The key advantage of this configuration over other FRET-based schemes is that the multi-modal emission of UCNPs allows for ratiometric sensing in which the relative intensities of two distinct peaks are compared rather than just the enhancement or quenching of a single one. Such ratiometric sensing reduces the sensing error due to variations in excitation intensity or nanoparticle concentrations, and thus makes these sensors much more robust against both sensor inhomogeneity and environmental noise [26].

However, FRET is not the sole process occurring that can affect the collected emissions. Unless a single UCNP can be measured directly, there exists a non-negligible chance that a photon emitted by one UCNP can be absorbed by a dye molecule on another nanoparticle. Such photon reabsorption (PR) would in turn lead to a decrease in the collected emission, thereby obscuring the true, localized FRET response of the original nanoparticle. An additional complication also arises from the fact that many of the visible UCNP emission lines originate from the same energy level. Since FRET acts as a decay pathway for an excited state electron, all emissions from this level should be affected equally by FRET, not just the one that overlaps with the dye's absorption band. To our knowledge, although the distinction between FRET and photon reabsorption has been discussed before [27, 28, 29], no FRET-UCNP sensor has yet been proposed that accurately accounts for these complications.

Arppe et al. [13], for example, measured the emission of pHrodo™ Red-succinimidly ester-conjugated UCNPs, but the observed dye emissions should result from both the local FRET and the global photon reabsorption. On the other hand, Ma et. al [16] demonstrated ratiometric sensing with 450 nm emission as the signal and 646 nm emission as the reference. However, the 646 nm emission originates from the same energy level as the 475 nm emission. The 646 nm emission, therefore, is FRET-sensitive and, when used as a reference in ratiometric sensing, cancels out the effect of FRET. While these papers showed that ratiometric sensing is possible with UCNPs, they did not properly separate the effects of photon reabsorption from those of FRET.

In this paper, we propose to accurately account for these intricacies by creating a FRET sensor via the conjugation of the pH-responsive dye Fluorescein Isothiocyanate (FITC) to a Thulium (Tm^{3+}), Ytterbium (Yb^{3+}) co-doped $NaYF_4$ UCNP. FITC is a well-known fluorescent dye that strongly absorbs 475 nm light. However, the magnitude of this absorption decreases with decreasing pH, thereby creating the dye's pH sensitivity. By

conjugating FITC to the UCNP surface, the distance between donor the Tm^{3+} ions and the acceptor dye molecules is small enough to have a strong FRET interaction. This FRET interaction in turn allows the pH sensitivity of FITC to be transferred to the UCNP emission [30] and thus allows the UCNPs to measure local pH. Unlike previous sensors that utilized FITC, we will show that using the 646 and 800 nm emissions avoids the spurious errors caused by both photon reabsorption and improper reference level choice, leading to a more accurate, localized FRET sensor.

2 Results

2.1 Theoretical analysis

As presented in the introduction, the measurement of local properties of a system such as pH, temperature, or pressure has attracted a lot of interest. Ratiometric UCNP-based sensing constitutes a promising solution but, if the spectral lines are not chosen carefully, the sensor signal can be affected by the photon reabsorption produced by other sensors present in the system. Similarly, measurements based exclusively on lifetime comparisons are usually slow, frequently rendering them an unfeasible option. In those occasions, ratiometric sensing based on intensity measurements constitutes the best solution. Here, we will present the rate equations analysis of a dye-coated UCNP-based sensor. The sensor will be designed to measure the effect of FRET while being robust against the consequences of non-local photon reabsorption and other environmental variations. We begin by analyzing the relevant energy levels of the dye-conjugated sensor (S2.1–5). These energy levels and transitions are shown in Figure 1. Briefly, the incident, 980 nm pump photons are absorbed by Yb^{3+} ions, which then transfer energy to the neighboring Tm^{3+} ions. If these energy transfer processes take place multiple times before the Tm^{3+} electrons decay, then the Tm^{3+} ions can emit luminescence at wavelengths shorter than the pump wavelength. This process is known as luminescence upconversion.

Specifically, emissions from the Tm^{3+} $^1G_4$ level result from a 3-photon upconversion process, while the emissions from the $^3H_4$ level correspond to a 2-photon process. Finally, there is FRET between the Tm^{3+} ions in the $^1G_4$ level and the FITC molecules coated on the UCNP surface. This process decreases both the intensity and lifetime of the emissions arising from the $^1G_4$ level. The strength of this FRET interaction depends on the dye's molar absorptivity. Thus, since the FITC absorbance depends on the pH, monitoring the intensity or lifetime change of the Tm^{3+} ions allows the sensing of local pH. Before we continue the discussion, it is noted that this analysis can be generalized to other dyes and dopants in a straightforward manner.

In order to perform a ratiometric measurement, a choice of two spectral lines is required. In particular, the signal line should be exclusively affected by FRET, whereas the reference line should not be affected by either FRET or photon reabsorption. The ratio of the intensities of those two lines would provide a FRET-based measurement independent of sensor concentration or any other environmental variations that influence the two intensities equally.

First, we can consider the intensities of the 475 nm and 646 nm lines, whose ratio has been identified in the past to report pH-sensitivity in sensors similar to the one described in this paper [10, 9]. The rate equation analysis given in the Supplementary Information (SI) shows that the intensity ratio is given as,

$$\frac{\Phi_{475}}{\Phi_{646}} = (1 - \alpha_{475})\frac{W_{30}}{W_{31}} \tag{1}$$

where Φ_{475} and Φ_{646} are the photon flux of 475 nm and 646 nm emissions respectively, α_{475} refers to the absorbance of the sensor at 475 nm, and W_{ij} is the radiative decay rate from level i to level j. From Figure 1, one can see that W_{30} and W_{31} are the radiative decay rates for 475 and 646 nm emissions, respectively. Note that the radiative decay rate is determined by the transition matrix element between the initial and final states and thus is not affected by FRET [31]. Therefore, a sensor based on the ratio of 475 and 646 nm emission intensities is not sensitive to FRET.

We can present this in an alternative way if we split the decay rate W_3 between its radiative and non-radiative components,

$$W_3 = W_3^{\text{rad}} + W_3^{\text{non-rad}} \tag{2}$$

where W_3^{rad} represents the total radiative decay rate, which is the sum of the transition rates for all radiative transitions originating from energy level $3(^1G_4)$. $W_3^{\text{non-rad}}$ is the total non-radiative decay rate, which contains the FRET rate between Tm^{3+} ions and FITC. The total radiative decay rate can be rewritten in terms of the radiative decay rate to a particular level j as $W_{3j} = \beta_{3j}W_3^{\text{rad}}$, where β_{3j} is the branching ratio from level 3 into the j-th level. Then, the ratio presented in equation 1 can be rewritten as:

$$\frac{\Phi_{475}}{\Phi_{646}} = (1 - \alpha_{475})\frac{\beta_{30}}{\beta_{31}} \tag{3}$$

Once again, since the branching ratio β_{ij} depends only on the transition matrix elements for the corresponding transitions [31, 32], the ratio given in Equation 1 is FRET-independent. In fact, the only variable that can change this ratio is the FITC absorbance α_{475}. This means that rather than measuring the local pH at the position of the sensor by FRET, this ratio is affected by the global amount of FITC present in solution. In other words, the mechanism behind previous reports of pH-sensitivity using this ratio of 475 and 646 nm intensities must be photon reabsorption.

To achieve truly local pH sensing based only on FRET and not on photon reabsorption, we propose, instead, to use the ratio $\Phi_{646}/\Phi 800$. In the steady state, weak pumping limit, we can derive the following ratio,

$$\frac{\Phi_{646}}{\Phi_{800}} = \frac{W_{31}}{W_3}\left[\frac{1}{W_{20}}\frac{c_3 N_{0'}}{W_{1'} + c_1 N_0}\right]\sigma\Phi \tag{4}$$

where, as indicated in Figure 1, W_i is the total (radiative and non-radiative) decay rate of the i-th level of Tm^{3+}, W_{ij} is the radiative decay rate between the i-th and the j-th levels of Tm^{3+}, $W_i^{'}$ is the total (radiative and non-radiative) decay rate of the i'-th level of Yb^{3+}, c_i is the energy transfer rate from Yb^{3+} to the i-th level of Tm^{3+}, N_i is the population of the i-th level of Tm^{3+}, $N_i^{'}$ is the population of the i level of Yb^{3+}, and $\sigma\Phi$ is the power absorbed by the Yb^{3+} ions doped in the UCNPs. A detailed derivation of this result and a description of the approximations used in order to obtain it, both in the weak and in the strong regimes, can be found in the Supplementary Information section S2.

The ratio Φ_{646}/Φ_{800} is FRET dependent because the total decay rate W_3 is dependent on the FRET rate as shown in Equation 2. All other parameters in equation 4 are not affected by pH. To show the FRET dependence explicitly, we can use Equation 2 and rewrite the ratio in front of the bracket in Equation 4 as:

$$\frac{W_{31}}{W_3} = \frac{\beta_{31}}{1 + W_3^{\text{non-rad}}/W_3^{\text{rad}}} \tag{5}$$

The effect of FRET is included in the variable $W_3^{\text{non-rad}}$, which may further be written as

$$W_3^{\text{non-rad}} = W_3^{\text{FRET}} + W_3^{\text{other}} \tag{6}$$

where W_3^{FRET} is the FRET rate and W_3^{other} is the total non-radiative decay rate due to any other mechanisms that may exist, e.g. multiphonon emission and energy transfer to defects. The FRET rate is strongly distance dependent. For dipole-dipole interactions, the distance dependence can be written in terms of the Förster radius, R_0[32],

$$W_3^{\text{FRET}} \propto \left(\frac{R_0}{r}\right)^6 \tag{7}$$

where r is the distance between the T^{3+} ion in the nanoparticle and the dye molecule on the nanoparticle surface; and R_0 is the Förster radius, defined as the distance at which the FRET rate equals the radiative decay rate. The sixth power of the Forster radius R_0^6, is directly proportional to the spectral overlap integral between the donor emission spectrum (here, the Tm^{3+} emission) and the acceptor molar extinction coefficient (here, the FITC absorption). As the absorbance of FITC changes with pH, so does the value of R_0, and

the degree of FRET experienced by the UCNPs. As a consequence, the ratio W_{31}/W_3 is sensitive to FRET between the ions and the dye, meaning that the Φ_{646}/Φ_{800} ratio is capable of recording local pH through FRET. It should be noted that, in order to accurately calculate the effect of FRET on the luminescence lifetime or intensity, one should integrate the FRET rates of various ions distributed within the volume of the nanoparticle [30]. The simple analysis presented here, however, is sufficient to show that the ratio Φ_{475}/Φ_{646} is not sensitive to FRET but the ratio Φ_{646}/Φ_{800} is. A similar analysis shows the ratio Φ_{475}/Φ_{800} is also sensitive to FRET. However, FITC absorbs at 475 nm and does not at 646 or 800 nm. Therefore, ratio measurements using 475 and 800 nm emission are subject to reabsorption of 475 nm luminescence by FITC molecules attached to other UCNPs. On the other hand, the Φ_{646}/Φ_{800} ratio is unaffected by the non-local photon reabsorption. Thus, ratiometric sensing with 646 and 800 nm emissions allows you to perform FRET-based sensing without being affected by photon reabsorption and therefore achieve truly local pH sensing.

2.2 Experimental observations

The theory outlined in the section above reveals that the spectral lines emitted from the same energy level are equally affected by FRET, whereas photon reabsorption affects only the lines whose wavelength overlaps with the dye absorption band. This means that it is possible to find an emission line that is affected by FRET but not by photon reabsorption. In particular, for the system of FITC-coated Tmdoped UCNPs described above, we observe that the:

- 475 nm emission is affected by both FRET and non-local photon reabsorption by FITC molecules on other UCNPs,
- 646 nm emission is affected by FRET in exactly the same way as 475 nm emission while being unaffected by photon reabsorption and,
- 800 nm emission is affected by neither FRET nor photon reabsorption.

To demonstrate these points, we first explored the possibility that photon reabsorption could be substantial enough to change the intensity of 475 nm emission. If this is the case, the 475 nm intensity should be dependent on the position of the sensor, or more precisely on the optical path length of the 475 nm luminescence signal within the solution. To test this theory, we performed the measurement described in Figure 2 (a). In this experiment, a near-infrared laser was focused on different spots within a pH 4 buffered solution of FITC-coated UCNPs. The luminescence signal was then collected perpendicular to the excitation, as indicated by the black arrow. For each one of the measurements, the optical path length within the solution was changed by translating the solution along the same direction the collection was performed.

As presented in Figure 2 (b), when the laser spot is close to the detector, the optical path length within the solution for the luminescence signal is short, and therefore the probability of photon reabsorption by other FITC molecules in the solution is small. The opposite is true when the laser spot is on the far side of the solution from the detector. Obviously, this photon reabsorption should happen only for the part of the UCNPs' emission spectrum that overlaps with the dye's absorption. Therefore, only the intensity of 475 nm emission

should be affected by this reabsorption, while the intensities of 646 and 800 nm should not be. In terms of ratios, Φ_{646}/Φ_{800} should be constant, while Φ_{475}/Φ_{646} should not be. The results presented in Figure 2 (c) agree with these expectations. The Φ_{475}/Φ_{646} ratio normalized to the first data point steadily decreased as the cuvette was moved closer to the detector, thereby increasing the optical path length for the luminescence signal to travel. In contrast, the normalized Φ_{646}/Φ_{800} ratio remained largely constant. The relative change in the Φ_{475}/Φ_{646} ratio was about 25% as the cuvette was moved by 2 mm. The changes in the Φ_{646}/Φ_{800} ratio remained within 5%.

To further confirm the observed effect is indeed due to photon reabsorption, we repeated the experiment presented in Figure 2 (b) with BF_4^- -coated UCNPs instead of FITC-coated UCNPs. Without any FITC present, there can be no FRET or photon reabsorption, and the Φ_{475}/Φ_{646} ratio should thus be constant. The results shown in Figure 2 (d) agree with this hypothesis. Once again, the Φ_{475}/Φ_{646} ratio from FITC-coated UCNPs showed a large and steady decrease with cuvette translation. But the same ratio from uncoated UCNPs remained mostly constant, with slight increase with cuvette translation. This effect was small compared to the large change observed with the FITC-coated UCNPs. Therefore, it does not impact our conclusion that the intensity of 475 nm emission and thus the ratio Φ_{475}/Φ_{646} change in the FITC-coated UCNP sample is caused by photon reabsorption. The severity of the non-local photon reabsorption will of course depend on the UCNP concentration and FITC density per nanoparticle. Nevertheless, the results presented in Figure 2 demonstrate that non-local photon reabsorption can be significant enough to obscure the local pH information provided by FRET.

Next, we performed time resolved photoluminescence (PL) spectroscopy to directly measure the effect of FRET. As shown in Equations 2 and 6, the total decay rate, which can be measured by the luminescence decay, depends on the FRET rate. Thus, as pH is increased, the absorbance of FITC should increase and consequently the FRET rate between Tm^{3+} and FITC should also increase. This should then manifest itself as a increase in the total decay rate, which is observable with time resolved PL measurements. One of the key insights from our theoretical analysis, as stated earlier, is that the 475 nm and 646 nm lines are equally affected by FRET. This conclusion follows naturally from the fact that the two emissions originate from the same energy level, $^1G_4$. In order to verify this conclusion experimentally, we excited FITC-coated UCNP solutions dispersed in different pH buffers with a pulsed laser (see SI Figure 5) and monitored the subsequent decay of luminescence intensity at various wavelengths. As shown in Figure 3, the decay of 475 and 646 nm luminescence decreases with increasing pH while the decay of 800 nm emission remains unchanged. More importantly, the decay of 475 and 646 nm emissions exhibit almost identical behavior as the solution pH is varied. To show this more clearly, we extracted the effective decay time by:

$$\tau_{\text{eff}} = \frac{1}{\Phi(0)} \int \Phi(t) dt \tag{8}$$

where $\Phi(t)$ is the luminescence intensity at a time t after the point of maximum intensity. The effective decay times for various luminescence lines as a function of pH is plotted in Figure 3 (d), which clearly shows that the decays of 475 and 646 nm emissions have identical behaviors while the decay of 800 nm is insensitive to pH. This confirms that the FRET interaction between the FITC molecules and the UCNP ions affects the 475 and 646 nm emissions in exactly the same way. As for the 800 nm lifetime, the dye's absorption for all the transitions involving the $^3H_4$ level is unaffected by pH, so it remains constant, independent of the choice of buffer solution.

We can actually quantify the difference in the effect of FRET observed for each one of the spectral lines if we calculate the relative change in lifetimes as the pH increases. In particular, the lifetime for the 475 nm line decreases by 17.2%, the lifetime of the 646 nm line decreases by 18.5%, and the lifetime of the 800 nm line decreases by 3.8%. That is, the $^1G_4$ energy level spectral lines relative change is four times bigger than that of the $^3H_4$ line.

Finally, to further show the agreement between the results presented by the rate equation modeling and the experiments, we performed steady-state PL measurements of FITC-coated UCNPs in different pH buffers. Since FRET is a non-radiative process that depopulates the emitting levels of Tm^{3+} ion, an increase of FRET rate results in an increase in the overall non-radiative decay rate, which in turn results in a decrease in luminescence intensity. Specifically, the luminescence intensity is proportional to quantum efficiency, which is given by:

$$\eta = \frac{\tau_{\text{rad}}^{-1}}{\tau_{\text{total}}^{-1}} = \frac{\tau_{\text{rad}}^{-1}}{\tau_{\text{rad}}^{-1} + \tau_{\text{non-rad}}^{-1}} \tag{9}$$

In our system, all luminescence lines have similar decay times as shown in Figure 3 (d). Therefore, the intensity ratios should be directly proportional to the ratios of total decay time which is given by the harmonic mean of radiative and non-radiative decay time and is measured by the PL decay experiments. Furthermore, since the decay time of 800 nm emission remains unchanged as the pH is varied, the ratio of decay times changes entirely due to the changes in the 646 nm decay time. Thus, we expect that the PL intensity ratio of 646 and 800 nm emissions will follow the behavior of decay time of 646 nm emission. These results are presented in Figure 4. As shown in Figure 4 (a), the PL intensity of 646 nm emission, when normalized to that of 800 nm emission, decreases with increasing pH. This, once again, is the consequence of enhanced FRET as the FITC absorbance increases with increasing pH. In Figure 4 (b), the intensity ratio Φ_{646}/Φ_{800} is plotted together with the relative changes in 646 nm lifetime. It clearly shows the intensity ratio tracks almost exactly with the changes in the lifetime of the 646 nm emission. This experiment confirms that the ratiometric sensing with 646 and 800 nm luminescence lines faithfully follows the changes in luminescence lifetimes due to FRET and therefore enables a truly local pH sensing based only on FRET. While the luminescence decay measurement is generally a more robust sensing method, intensity ratio measurement is usually easier to implement and therefore more widely applicable.

3 Conclusion

Dye-coated UCNPs constitute some of the most promising FRET-based sensors. In addition to many advantages of UCNPs such as no blinking, no photobleaching and no background autofluorescence, this sensor configuration can also exploit the multiple spectral lines UCNPs emit. This multi-color emission enables ratiometric measurements, which are much more robust to environmental noise. However, in order to achieve truly local sensing, the interplay between the two mechanisms that can affect the sensor signals, FRET and photon reabsorption, must be clearly elucidated.

Since FRET is a highly localized process, its effect quickly becomes negligible as the distance between the dye molecules and the UCNP ions increases. Therefore, it can be used to properly sense the local properties of a system. In contrast, photon reabsorption can occur anywhere in the sample volume and thus leads to a global response. As we have shown in this paper, it is not sufficient to simply take the ratio between a line that is affected by FRET and one that is not. Many emission lines that experience FRET are also affected by photon reabsorption, and non-local photon reabsorption can obscure the local response provided by FRET.

Through an experimentally-corroborated rate equation analysis, we have shown that multiple spectral lines emitted by the same energy level are equally affected by FRET, making it possible to choose spectral lines that are FRET-dependent but protected against photon reabsorption. By pairing one of these spectral lines with another emission line that is affected neither by FRET nor by photon reabsorption, we can implement a ratiometric sensing mechanism that responds only to local pH.

In order to experimentally explore that possibility, we have used a set of FITC-coated UCNPs. We have shown that, in a system using $NaYF_4:Yb^{3+},Tm^{3+}$ UCNPs, the 475 nm intensity depends on both FRET and photon reabsorption, the 646 nm intensity is sensitive only to FRET, and the 800 nm intensity is affected by neither. Therefore, the ratio Φ_{646}/Φ_{800} is dependent only on FRET and not on photon reabsorption, allowing for a truly local pH sensing. We have also shown that the ratio Φ_{475}/Φ_{646}, which has been commonly used in the literature, is susceptible to photon reabsorption and cannot accurately measure FRET.

To our knowledge, this constitutes the first FRET-based UCNP sensing scheme that accurately accounts for the complications that may arise from non-local effects in a real system. The strategy is readily applicable to any FRET-based UCNP sensing and can thus impact a wide range of biosensing applications.

4 Experimental Details

4.1 Sensor Fabrication

A detailed description of the fabrication of the FRET-based sensor can be found in the supplementary information. Briefly, oleic acid-coated UCNPs were synthesized, followed by ligand exchange with polyethylenimine (PEI) to render them dispersible in water. Finally, FITC was conjugated to the PEI ligands via formation of an amide bond.

4.2 Materials Characterization

A representative TEM image of the synthesized OA-coated UCNPs is shown in Figure 5 along with their corresponding size distribution. The nanoparticles are monodispersed, with an average size of 29.3 ± 2 nm. After conjugation with the FITC dye molecules, colloidal stability was tested via Dynamic Light Scattering (DLS). At pH 4, the particles are strongly stabilized by the large positive charge of the protonated amines in PEI, and the corresponding hydrodynamic diameter was found to be 115.9 ± 34.2 nm. The diameter at pH 5 was also 126.6 ± 31.6, indicating strong colloidal stability in acidic environments. However, as the pH of the solution increases, the particles become more unstable due to the decreasing amount of positive charge on the PEI amines. While the FITC molecules actually become more charged at higher pH, the relatively small amount of dye molecules compared to the ligand polymer ensures that the PEI characteristics dominate. The decreased stability in turn causes concentration inhomogeneity, which makes sensor calibration at higher pH values difficult (i.e. pH 6 or higher). This phenomenon is not unique to our system, as Mahata et al. [10] found an average hydrodynamic size of 1491.5 ± 221.7 for a similar FITC/PEI-UCNP system at pH 6. Such concentration variability further highlights the need to ensure that the UCNP sensor characteristics depend exclusively on local characteristics and not on global effects.

To determine the number of FITC molecules on the UCNP surface, we originally tried to estimate this amount via quantitative UV-Vis, but particle instability (especially at the physiological pHs), prevented this from occurring. In our previous paper (see reference [30]), we were able to quantify FITC loading by measuring the FITC absorption with FITC-UCNPs dispersed in DMF, in which the particles are significantly more stable. In this work, the consistency of optical properties from sample to sample suggests that the FITC loading is similar to that reported in reference [30].

4.3 Instrumentation

Transmission electron microscopy (TEM) images of the UCNPs were obtained using a Tecnai T12 Spirit 120 kV Electron Microscope. The particle diameter distribution was calculated using ImageJ software to determine particle area. At least 200 particles were used to calculate the size distribution. Dynamic Light Scattering (DLS) measurements were collected via an Anton-Paar Litesizer. All DLS data shown in this paper is calculated using only intensity due to uncertainty in the appropriate refractive index. Note that no filtration was used for DLS, in order to gain the most accurate picture of the solution dynamics. A J-Kem Scientific 210 temperature controller was used to regulate the temperature during the nanoparticle synthesis.

Transient photoluminescense (PL) measurements were performed by modulating an excitation laser source (Thorlabs L980P200) with a rectangular pulse generated by a function generator (Wavetek model 166). The power density of the 0.8 ms laser pulse was 1 kW/cm^2. The duty ratio was set appropriately so that the transient PL had enough time to reach the steady state. Here, we defined a period of 10 ms. Between 10^5 and 5×10^5 pulses were accumulated in order to obtain the results presented in Figure 3.

The emitted PL from the solutions was then collected with a convex lens and imaged by a 4f system of lenses into a monochromator (Sciencetech 9057F) equipped with a visible photomultiplier tube (Hamamatsu H11461P-11 PMT). Finally, a photon counter (Stanford Research Systems SR430) was used to convert the photomultiplier tube's output to digital transient waveforms that were recorded and post-processed using our custom software.

The ratiometric measurments were performed with a similar setup, but they were collected with a spectrometer with cooled charge-coupled device detectors (Acton SpectraPro 300i). The spectra was optically filtered by using Edmunds Optics' short-pass 900 nm filter, and a long-pass 450 nm filter.

Supplementary Material

Refer to Web version on PubMed Central for supplementary material.

Acknowledgements

This work was supported in part by the National Science Foundation (NSF) (Nos. DMR-1420736 and CBET 2029559) and National Institute of Health (NIH) (1 R21 GM140347).

References

[1]. Webb BA, Chimenti M, Jacobson MP, Barber DL, Nat. Rev. Cancer 2011, 11 671. [PubMed: 21833026]

[2]. Wang Y, Zhou K, Huang G, Hensley C, Huang X, Ma X, Zhao T, Sumer BD, DeBerardinis RJ, Gao J, Nat. Mater 2014, 13 204. [PubMed: 24317187]

[3]. Bunt G, Wouters FS, Biophys. Rev. (Heidelberg, Ger.) 2017, 9 119.

[4]. Algar WR, Hildebrandt N, Vogel SS, Medintz IL, Nat. Methods 2019, 16 815. [PubMed: 31471616]

[5]. Hildebrandt N, FRET–Foerster Reson. Energy Transfer 2013, 105–163.

[6]. Ostrowski AD, Chan EM, Gargas DJ, Katz EM, Han G, Schuck PJ, Milliron DJ, Cohen BE, ACS Nano 2012, 6 2686. [PubMed: 22339653]

[7]. Cheng L, Yang K, Zhang S, Shao M, Lee S, Liu Z, Nano Res. 2010, 3 722.

[8]. Li H, Dong H, Yu M, Liu C, Li Z, Wei L, Sun L-D, Zhang H, Anal. Chem. (Washington, DC, U. S.) 2017, 89 8863.

[9]. Li C, Zuo J, Zhang L, Chang Y, Zhang Y, Tu L, Liu X, Xue B, Li Q, Zhao H, Zhang H, Kong X, Sci. Rep 2016, 6 1. [PubMed: 28442746]

[10]. Mahata MK, Lee KT, Nanoscale Adv. 2019, 1 2372. [PubMed: 36131991]

[11]. Du S, Hernández-Gil J, Dong H, Zheng X, Lyu G, Bañobre-López M, Gallo J, Sun L.-d., Yan C.-h., N. J. Long, Dalton Trans 2017, 46 13957.

[12]. Wu Y-X, Zhang X-B, Zhang D-L, Zhang C-C, Li J-B, Wu Y, Song Z-L, Yu R-Q, Tan W, Anal. Chem. (Washington, DC, U. S.) 2016, 88 1639.

[13]. Arppe R, Näreoja T, Nylund S, Mattsson L, Koho S, Rosenholm JM, Soukka T, Schäferling M, Nanoscale 2014, 6 6837.

[14]. Liu X, Zhang S-Q, Wei X, Yang T, Chen M-L, Wang J-H, Biosens. Bioelectron 2018, 109 150. [PubMed: 29550738]

[15]. Näreoja T, Deguchi T, Christ S, Peltomaa R, Prabhakar N, Fazeli E, Perälä N, Rosenholm JM, Arppe R, Soukka T, Schäferling M, Anal. Chem. (Washington, DC, U. S.) 2017, 89 1501.

[16]. Ma T, Ma Y, Liu S, Zhang L, Yang T, Yang H-R, Lv W, Yu Q, Xu W, Zhao Q, Huang W, J. Mater. Chem. C 2015, 3 6616.

[17]. Chen E, Cai K, Liu X, Wu S, Wu Z, Ma M, Chen B, Zhao Z, Anal. Chem. (Washington, DC, U. S.) 2021, 93 6895.

[18]. Meier RJ, Simbürger JM, Soukka T, Schaferling M, Anal. Chem. (Washington, DC, U. S.) 2014, 86 5535.

[19]. Wu J, Qin Y, Sens. Actuators, B 2014, 192 51.

[20]. Xie L, Qin Y, Chen H-Y, Anal. Chem. (Washington, DC, U. S.) 2013, 85 2617.

[21]. Tsai ES, Himmelstoß SF, Wiesholler LM, Hirsch T, Hall EA, Analyst (Cambridge, U. K.) 2019, 144 5547.

[22]. Mader HS, Wolfbeis OS, Anal. Chem. (Washington, DC, U. S.) 2010, 82 5002.

[23]. Esipova TV, Ye X, Collins JE, Sakadžić S, Mandeville ET, Murray CB, Vinogradov SA, Proc. Natl. Acad. Sci. U. S. A 2012, 109 20826.

[24]. Strobl M, Mayr T, Klimant I, Borisov SM, Sens. Actuators, B 2017, 245 972.

[25]. Laguna M, Escudero A, Núñez NO, Becerro AI, Ocaña M, Dalton Trans. 2017, 46 11575.

[26]. Bae K, Xu B, Das A, Wolenski C, Rappeport E, Park W, RSC Adv. 2021, 11 18205.

[27]. Bhuckory S, Hemmer E, Wu Y-T, Yahia-Ammar A, Vetrone F, Hildebrandt N, Eur. J. Inorg. Chem 2017, 2017 5186.

[28]. Rojas-Gutierrez PA, Bhuckory S, Mingoes C, Hildebrandt N, DeWolf C, Capobianco JA, ACS Appl. Nano Mater. 2018, 1 5345.

[29]. Francés-Soriano L, Peruffo N, Natile MM, Hildebrandt N, Analyst (Cambridge, U. K.) 2020, 145 2543.

[30]. Das A, Corbella Bagot C, Rappeport E, Ba Tis T, Park W, J. Appl. Phys. (Melville, NY, U. S.) 2021, 130 023102.

[31]. Tanabe S, Tamai K, Hirao K, Soga N, Phys. Rev. B 1996, 53 8358.

[32]. Bednarkiewicz A, Chan EM, Prorok K, Nanoscale Adv. 2020, 2 4863. [PubMed: 36132913]

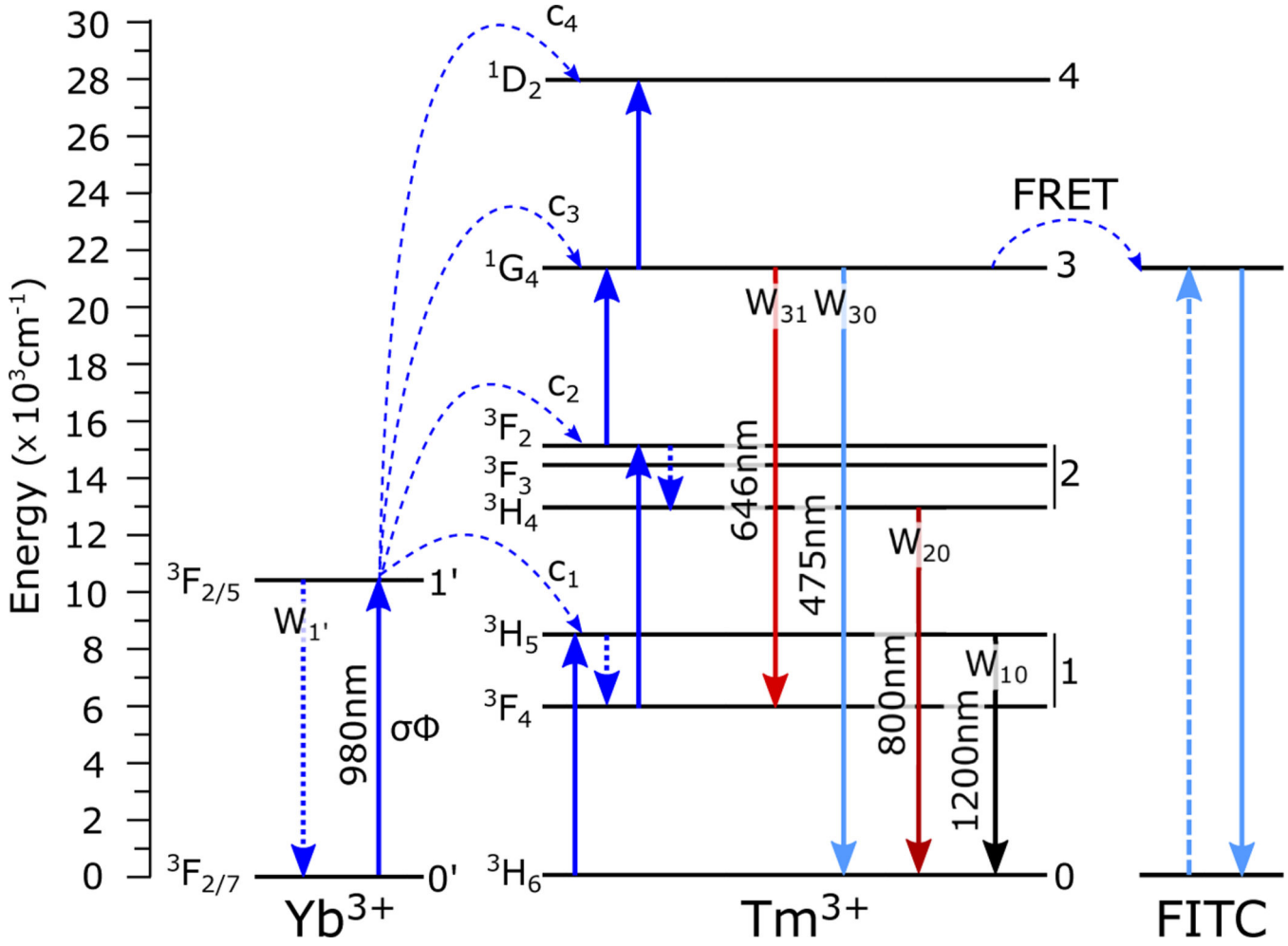

Figure 1:

Tm^{3+}, Yb^{3+} co-doped upconverting nanoparticles energy level diagram. The UCNPs' Yb^{3+} ions absorb 980 nm light, transferring that energy into its neighbouring Tm^{3+} ions. If the decay rate of the intermediate levels is slow enough that several photons' energy can be transferred into Tm^{3+} before its energy is released, then the population of higher energy levels in Tm^{3+} will increase. At that point, some of this energy will be non-radiatevely transmitted into FITC via FRET, and some will be emitted radiatively. The emissions relevant to the discussion presented in section 2.1 are marked in the diagram, with their characteristic wavelength indicated next to the arrow.

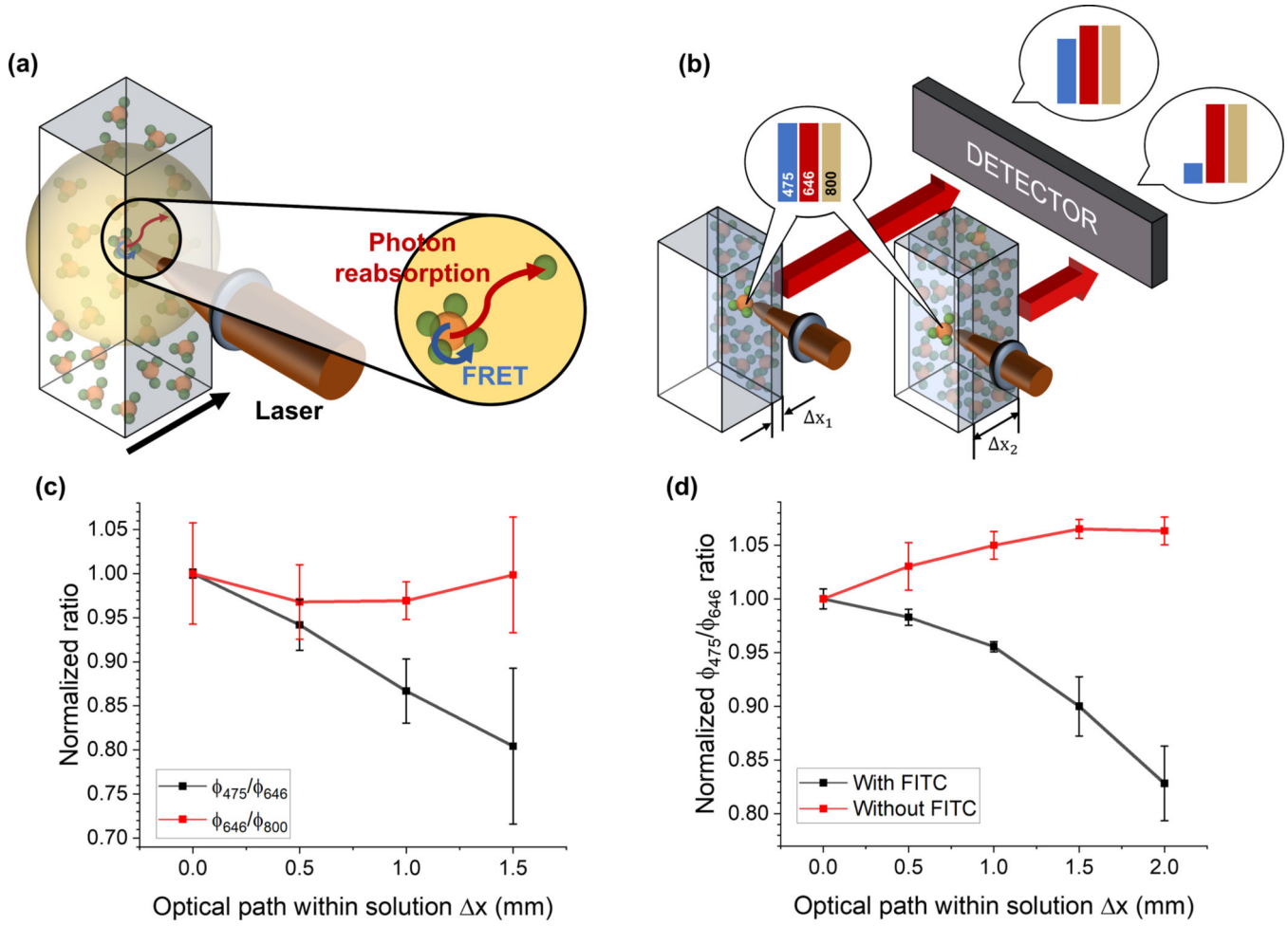

Figure 2:

(a) While FRET is a local phenomena, part of the upconversion luminescence from the nanoparticles can be absorbed through photon reabsorption by dyes that are not coated on the UCNP that produced it. This phenomena might obscure the results of a ratiometric measurement. **(b)** Schematic of the experimental setup. A solution of UCNPs coated with FITC is placed inside a cuvette. The cuvette is moved, changing the length of the optical pathway within the solution. As indicated, the UCNPs emit photons with different wavelengths. Assuming the solution is homogeneous, the intensity of the UCNPs' emission should be independent from the position of the cuvette. As the FITC present in the solution absorbs 475 nm intensity, we would expect that the more solution the photoluminesce needs to go through in order to reach the detector, the less 475 nm intensity that gets detected. Emitted and detected intensities are presented in the drawing with colored bars with a height directly proportional to the intensity they represent. **(c)** Results from the experiment presented in (b). As the laser incidence point in the cuvette gets closer to the detector, the intensity ratio Φ_{475}/Φ_{646} increases because the photon reabsorption effect becomes smaller. Φ_{646}/Φ_{800} remains almost constant in the central part of the cuvette. Outside of that region, the power dependence of the ratio Φ_{646}/Φ_{800} becomes an issue, as outlined in the Supplementary Information. **(d)** A solution of BF_4^- -coated UCNPs (black) and a solution of FITC-coated

UCNPs (red) are placed inside a cuvette in pH 4 buffer. Following the idea outlined in subfigure (b), the cuvette is moved, changing the length of the optical pathway within the solution. Since the FITC present in the solution absorbs part of the 475 nm intensity, the Φ_{475}/Φ_{646} ratio decreases as we increase the amount of solution the photoluminescence needs to go through before it reaches the detector.

All sets of data have been normalized to their first value to facilitate comparison. 2mg/mL solutions of FITC- and BF_4^- coated UCNPs were used for the experiments in (c), (d).

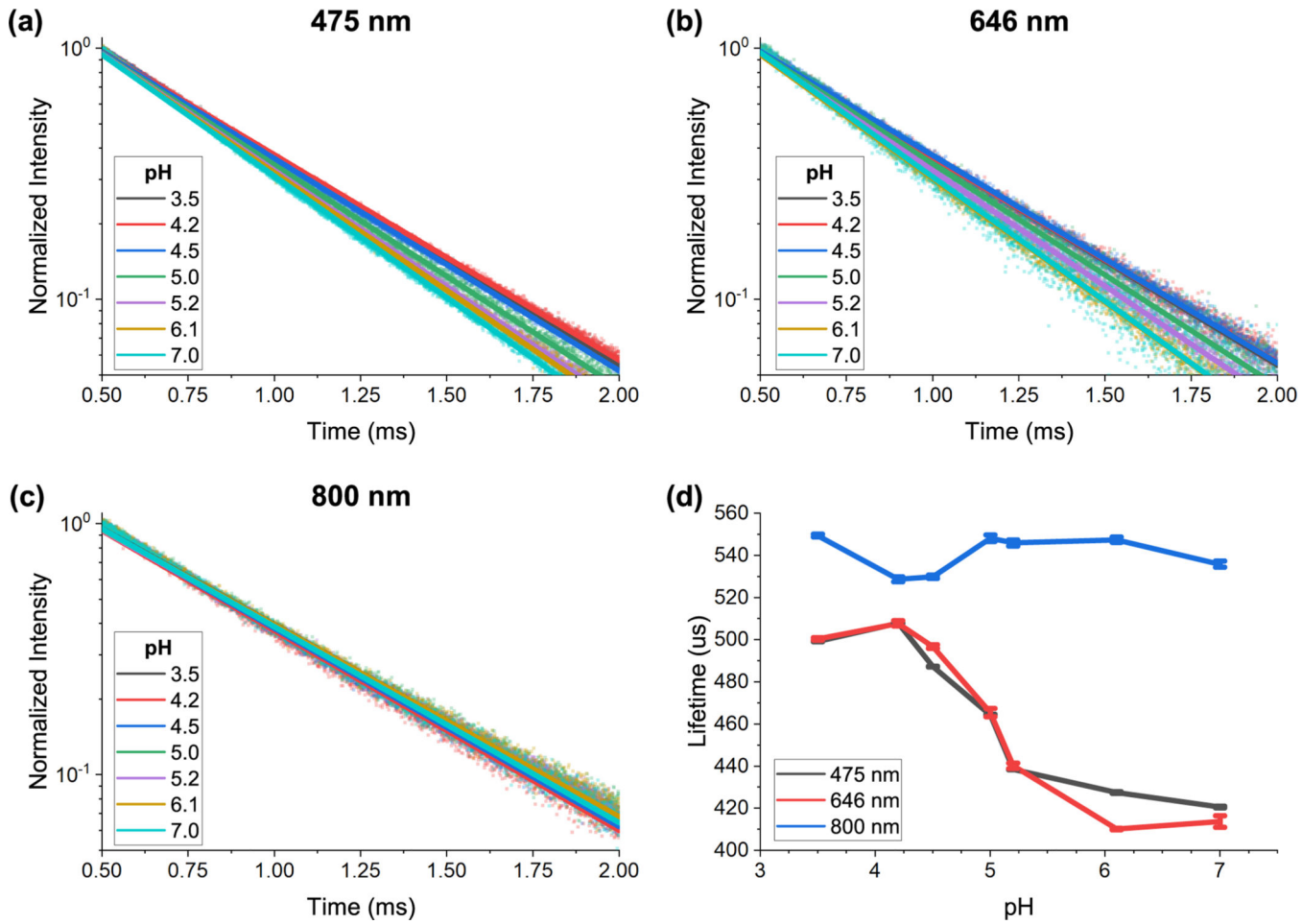

Figure 3:

(a-c) Time decay measurement profiles for three of the FITC-coated UCNPs emission lines, in different pH buffers. **(d)** Effective lifetimes obtained by integration of the time decay measurements presented in this figure's subplots (a-c). The uncertainty estimation procedure is described in detail in the Supplementary Information section S3. The 800 nm lifetime remains constant whereas the 475 and 646 nm lifetimes become smaller as the pH increases. The change in the lifetime for the 475 and 646 nm spectral lines becomes smaller as the pH increases, and is negligible between the sample in the pH 3.5 buffer and that of the pH 4 buffer.

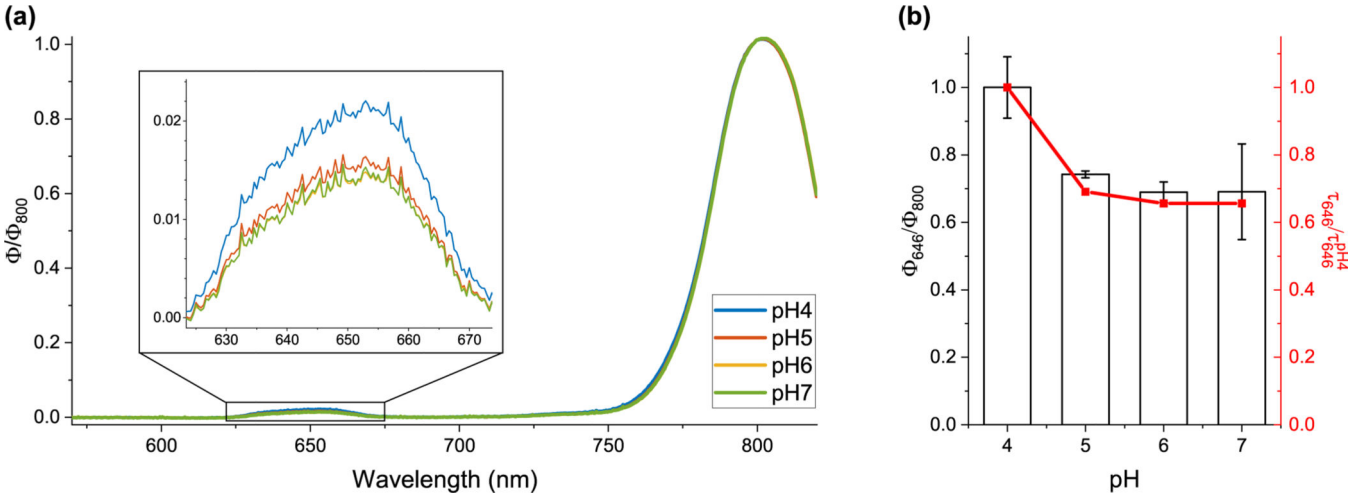

Figure 4:

(a) Normalized photoluminescense spectra of FITC-coated UCNPs. As the pH increases, so does FITC's absorption, decreasing the intensity detected for the 646 nm spectral line. **(b)** Φ_{646}/Φ_{800} (in black) and τ_{646} (in red), normalized to the value obtained in the pH 4 buffer. We observe that the ratio between the intensities at 646 nm and 800 nm tracks the lifetime decrease of the 646 nm line as the pH increases. We also notice an increase in the standard deviation of the measurements as the pH of the solution approaches 7. A discussion on the instabilities of the FITC-coated UCNPs at those pHs can be found in the Materials Characterization section.

Three independently prepared FITC-coated UCNP solutions were measured in this experiment. Subfigure (a) shows the average of these three measurements, and subfigure (b) presents both the average and the spread of those measurements.

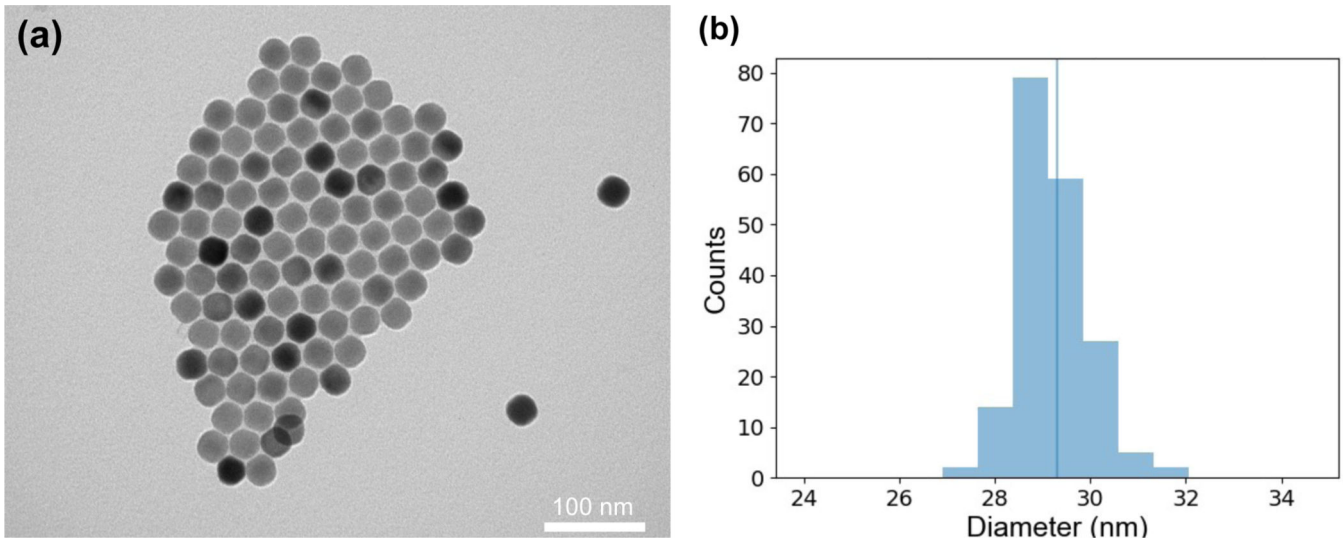

Figure 5:

(a) Representative TEM image of the as-synthesized OA-coated UCNPs. Scale bar denotes 100 nm. **(b)** Size distribution of the synthesized nanoparticles. The average diameter was found to be 29.3 ± 2.0 nm.